Chapter 5

On the Mechanical and Dielectric Properties of Biocomposites Containing Strontium Titanate Particles

Amarilis Declet-Vega, Nelson Sepúlveda-Ramos and Oscar Marcelo Suárez

Additional information is available at the end of the chapter

http://dx.doi.org/10.5772/intechopen.76858

Abstract

In recent years, scientists advanced the study of bio-ferroelectric composites to develop new environmentally friendly and inexpensive electronic elements such as capacitors, actuators, and transistors. Accordingly, the present research relates to composites made of chitosan-cellulose polymeric matrix and strontium titanate (STO) nanoparticles. The variables considered include different percentages of cellulose (15 and 25 v%) and strontium titanate nanoparticles (10 and 20 wt%). The electrical characterization of the composites included measuring their dielectric constant, current density, and conductivity. The results suggest that the addition of STO nanoparticles raised the dielectric constant while lowering the current density and the conductivity of the nanocomposites. Moreover, although the cellulose addition increased the current density and the conductivity of the composites, it lowered their dielectric constant. Also, the resulting biocomposite capacitors could withstand up to 60 V without any detectable dielectric breakdown. The other two properties measured were the ultimate tensile strength (UTS) and the degradation temperature (Tdeg). Higher percentages of cellulose decreased the UTS and the Tdeg of the chitosan-cellulose composites while the addition of cellulose slightly raised these properties of the composites made of chitosan-cellulose and STO nanoparticles. The results proved that these types of biocomposites are apt as capacitors with adequate strength to withstand aggressive environments. This work was fully conducted in the facilities of the Nanotechnology Center hosted by the University of Puerto Rico – Mayagüez, from December 2014 to January 2017.

Keywords: ferroelectric nanoparticles, dielectric constant, biopolymers, chitosan, biocomposites, strontium titanate

1. Introduction

Biopolymers have attained significant market potential due to their numerous applications in diverse fields such as "bio-ceramic, bio-sensing, bio-encapsulation, and bio-inorganic nanoparticles" [1]. The main motivation for studying these biopolymers rises from their unique characteristics: bio-compatibility, low environmental impact, and nontoxicity (for human use) [2, 3]. Since these materials are biodegradable, they can be recycled, which translates into waste reduction and smaller recycling cost. An additional appealing feature is the low fabrication cost of these biopolymers when compared to petroleum-based ones.

Researchers have been using these biopolymers as matrices for composites containing ferroelectric particles, i.e., $BaTiO_3$, $SrTiO_3$, $CaTiO_3$, and $PbTiO_3$. In particular, they have been seeking for an alternative for processable high permittivity materials with high dielectric constant, moderate dielectric strength, low dielectric loss, high electrical resistivity, among other properties [4, 5]. These electrical characteristics made these composites particularly suitable for capacitors, transistors, and actuators.

For instance, Neagu et al. studied dielectric properties of bio-composites made of chitosan with different percentages of $BaTiO_3$ particles: 0, 1 and 10% [6]. Among the different fabrication methods available to produce the polymeric films, the authors selected the dry phase inversion casting process. This research demonstrated that higher $BaTiO_3$ concentrations in the polymeric matrix raised the dielectric constant while lowering the dielectric loss. This led to a simple approach to create flexible electronic devices made of polymeric and ferroelectric constituents.

Moreover, Elimat evaluated the electrical properties of composites made of epoxy with various zinc oxide (ZnO) concentrations and reinforced with 1.0 wt% of conductive carbon black nanoparticles to dissipate any potential electrostatic charges [7]. The results revealed an increase in higher dielectric constant values as the temperature and the ZnO concentration heightened. However, that dielectric constant diminished for higher frequencies, namely from 0.1 to 1 MHz; this was attributed to the dipoles' lack of time to align with the electrical field. In addition, the authors demonstrated that higher concentrations of ZnO nanoparticles increased the electrical conductivity of the composites. Such higher electrical conductivity is due to the increase of the charge carriers' density in the polymeric matrix.

Petrov et al. studied the electrical properties of chitosan and hydroxyapatite (HA) bio-composites. In their study, they implemented an innovative approach via a corona discharge treatment to increase the charge surface of the polymeric matrix. The researchers tested the dielectric permittivity of the composites using dielectric spectroscopy and by employing a parallel plate capacitor for the electrical measurements. Their results evinced no difference in dielectric permittivity between the composites made of 6 and 10 g/L of chitosan solution. However, a notable difference was observed in the dielectric permittivity as a function of temperature and frequency. Although higher temperatures increased the dielectric permittivity of the composites, such permittivity decreased at higher frequencies [8].

Hosokawa et al. fabricated composites made of chitosan and cellulose to study their mechanical properties [9]. To fabricate the composites, chitosan was dissolved in a water/acetic acid while cellulose fibers were diluted in an aqueous solution. Then, a small amount of chitosan was added into the cellulose solution containing glycerol. The ensuing solution was mechanically stirred and degassed before the drying process. Their results suggest that the tensile strength decreased as the swelling degree increased in the composites. The authors attributed this to the crosslinking between the carbonyl groups (C═O) and the carbonyl groups (C–OH) in the cellulose structure with the amine groups of the chitosan.

Another pertinent study was conducted by Ibrahim et al., who fabricated polyester-oil palm ash composites [10]. The specimens were prepared at different volume fraction of oil palm ash (0, 10, 20 and 30%) in unsaturated polyester matrix. All samples were mechanically characterized with a universal testing machine with a 10 kN load capacity, operated at a 5 mm/min strain rate. The measured tensile strength of the composites decreased from 26.8 to 13 MPa with the tensile modulus rising from 375 to 499 MPa as the content of nanofillers increased from 0 to 30%. The smaller tensile strength was attributed to the interaction of the nanofiller with the polymer matrix. Conversely, the fillers imparted greater stiffness to the composite. In addition, when the authors analyzed the composites' thermal properties, they discovered that the particles enhanced the thermal stability of the composites from 293.55°C without oil palm ash to 401.72°C with 30% oil palm ash.

Aware of such trend and in an effort to propose an alternative material suitable for capacitors, in the present research we engineered a composite with a chitosan-cellulose matrix, reinforced with strontium titanate ($SrTiO_3$) nanoparticles. The polymeric matrix provides flexibility, which is adjustable with the relative amount of cellulose, while the $SrTiO_3$ (STO) nanoparticles helped tune the dielectric constant, the current density, and the electrical conductivity. The control of the capacitance dependency on the frequency would allow devices to vary their capacitance depending on the application in which they would be deployed. Hence, this work brings about a novel perspective on the tunable properties of the chitosan-based composite for flexible electronics and bio-compatible properties.

2. Experimental procedure

The present research encompassed two stages. In the first one, the composites were synthesized to produce enough material for the second stage. Upon this stage, the composites underwent both mechanical and electrical characterization. This experimental section was completed in the facilities of the Nanotechnology Center hosted by the University of Puerto Rico – Mayagüez, from August 2013 to August 2015.

2.1. Materials selection

All samples were fabricated using poly (D-glucosamine) deacetylated chitosan ($(C_6H_{11}O_4N)_n$, 75% deacetylation, Sigma Aldrich), cellulose powder (cotton linens, Sigma Aldrich) and strontium titanium oxide (($SrTiO_3$), 99 + %, Fisher). A chitosan solution was dissolved in acetic

acid solution (CH_3CO_2H, 99.7 + %, Alfa Aesar) while 4-methylmorpholine N-oxide solvent (CH_3CO_2H, 99.7 + %, Alfa Aesar) was needed to dissolve the cellulose powder. The fabrication of the composites consisted of two subsequent stages: (1) fabrication of chitosan-cellulose films, and (2) synthesis of chitosan-cellulose composites containing $SrTiO_3$ nanoparticles.

2.2. Sample preparation

To prepare the specimens, one must considered their adequate size for the ensuing characterization. In particular, special care was taken to better the uniform distribution of the particles in the matrix.

2.2.1. Biopolymeric films

The biopolymeric films consisted of a mixture of chitosan and cellulose, prepared by means of the solution casting technique. To prepare the chitosan solution, a fixed concentration of the polymer (1.5 v%) was dissolved in an acetic acid aqueous solution and mechanically stirred. Furthermore, the cellulose solution was made by adding the polymer into a 4-Methylmorpholine N-oxide (NMMO) solvent, followed by mechanical stirring at 65°C to enhance the polymer solubility. A fixed concentration of cellulose, i.e., 0.5 v%, was used for the preparation of the composites. A higher concentration of cellulose would have raised the water content, which could have been detrimental for the resulting electrical, mechanical, and thermal properties.

After the stock solutions of chitosan and cellulose were prepared separately, we readied smaller stock solutions with different volume percentages of chitosan and cellulose: 85 v%Ch-15 v%Cel and 75 v%Ch-25 v%Cel. After mixing the components, we mechanically stirred the solutions, poured them into petri dishes, and let them dry in an oven at 40°C. Afterwards, we removed the films from the petri dishes using a basic solution and dried them in an oven once again [7].

2.2.2. Bio-ferroelectric nanocomposites

The double layered bio-ferroelectric composites were fabricated layer-by-layer via the solution casting method. The first layer consisted of chitosan-cellulose bio-polymers and the second layer consisted of the bio-polymers mixed with strontium titanate (STO) particles. To fabricate the said first layer, small solutions of chitosan and cellulose (i.e., 85 v%Ch-15 v%Cel and 75 v%Ch-25 v%Cel) were synthesized and transferred in the petri dishes for the dry process. The purpose of the second layer was to prevent the nanoparticles from settling and passing through the still soft first polymeric film. Hence, for the second layer, the same amount of small solutions was synthesized, this time with different STO amounts, i.e., 10 and 20 wt%; the goal was to analyze their effect in the electrical properties of the resulting biocomposites. Thereafter, these solutions were transferred onto their corresponding first layer of chitosan-cellulose followed by a second drying process to remove any residual water from the polymeric matrix.

The dispersion of nanoparticles within a given matrix has always been an issue, as proven in a prior research [11]. Therefore, to enhance such dispersion in the matrix we reduced the size of the particles using a varioplanetary high energy ball mill. To find the optimal time in which

we could reduce the particle size to the smallest possible, the particle size was determined at different milling times using the Scherrer equation [12, 13]. Afterwards, the particle size was computed at different milling times to select the most time-efficient operation, i.e., maximum size reduction at minimal time. The overall technique had been successfully implemented to reduce the size of compound particles in previously published works [14, 15].

2.3. Characterization

2.3.1. Structure analysis

All samples were characterized with a Rigaku ULTIMA III diffractometer operated at 40 kV and 44 mA. The characterization of the composites was conducted at 25°C with a 2θ step of 0.02° and a 1 s dwelling time. The target used was copper with a Kα wavelength of 0.154178 nm.

2.3.2. Electrical analysis

To measure the capacitance of the composites, we utilized a QuadTech 2200 automatic transformer system (with an AC supply). The frequency range was set from 1 to 10 kHz. Once the capacitance readings as a function of the frequency were recorded, the dielectric constant was determined for the biocomposites using Eq. (1).

$$K = \frac{C.d}{A.\varepsilon_0} \tag{1}$$

where K is the dielectric constant; C, the capacitance of the dielectric material; A, the area of the plates; d, the distance between the plates; and ε_o, the permittivity of vacuum [16].

To study dielectric breakdown in the composite, a GW INSTEK GPS-3303 DC power supply provided the current passing through the material when the applied voltage changed from 5 to 60 V. A GW-INSTEK GDM-8246 power meter connected in series was used to register the current values by following the guidelines of the ASTM D-149 standard [17]. According to this standard, the current flow must be recorded at equal increments of voltage and after a specific time. For our research, 5 V increments were applied to the dielectric material and then, after 10 s, the current flow was recorded at each of those increments. The current allowed us to determine the conductivity of the dielectric material.

To construct the capacitor, an AJA ATC Orion magnetron sputtering unit permitted to apply a titanium coating on both sides of the biocomposite film for 20 min at 200 W. All these capacitors were characterized using a Caframo™ stirrer clamp made of cast zinc-aluminum alloy and coated with epoxy as shown in **Figure 1**. The stirrer clamp also included a hold chuck key to ensure a close circuit between the capacitor and the copper electrodes. One electrode was placed at the base of the chuck key while another electrode was placed at the base of the Calframo™ stirrer clamp. In addition, a small weight of 1.27 N was placed on top of the chuck key to ensure proper contact between the capacitor and the electrodes. The ASTM D-150 standard provided guidelines to select the dimensions of the capacitors, i.e., 10 mm in length and 10 mm in width [18, 19].

Figure 1. Calframo™ stirrer clamp utilized in the measurement of the dielectric properties.

2.3.3. Thermal analysis

A Mettler Toledo TGA/SDTA thermogravimetric / differential thermal analyzer (operated at a 5°C/min. Temperature ramp from 25 to 500°C) allowed determining the degradation temperature (T_{deg}) of the composites in a nitrogen atmosphere. The samples were placed on a weight scale, which detects the mass loss of the samples as a function of temperature. To determine the said T_{deg}, the first derivate was applied to the heating rate curve obtained from the thermal analyzer.

2.3.4. Mechanical characterization

The samples' ultimate tensile strength was measured at room temperature (25°C) using a low force Instron® model 5944 universal testing machine. The deformation velocity was set at 1 mm/min. Also, the dimensions of the samples followed the ASTM D-1708, which specifies a 22 mm gauge length, a 5 mm width, and a 5 mm radius fillet.

3. Results and discussion

3.1. $SrTiO_3$ Nanoparticles

Previous research showed that the particle size affects electrical, mechanical, and thermal properties of similar composites [20]. As aforementioned, to improve the dispersion of the particles in the polymeric matrix, the particle size was reduced using the high energy ball mill.

Furthermore, reducing the size of the particles can create impurities upon ball milling and to confirm that the crystalline structure of the strontium titanate remained without changes, the powder was analyzed by x-ray diffraction. **Figure 2** displays the resulting diffractogram that matched with the expected STO pattern; the presence of impurities was not detected.

As aforementioned, from the diffractograms, Scherrer equation allowed estimating the particle size of the STO powder at different milling times. The equation takes into consideration the width of the largest XRD peak in the diffractogram [21, 22], which in our case (**Figure 2**) lies at $\theta = 32.5°$. The Miller indexes were identified by comparison with a prior publication by Trepakov et al. [23].

Figure 3 presents the milling time effect on the particle size. Two stages can be observed in the reduction (by fragmentation) of the particle size. The first stage occurs between 0 to 5 h of milling and presents a rapid reduction in the particle size from 46 to 18 nm. The rapid reduction in the particle size may be attributed to the fragmentation of large agglomerates into individual aggregates and therefore, the fracture of aggregates into individual primary particles and small aggregates [24]. In the second stage (5–20 h) of milling, the change in size was negligible. This was attributed to the increasing agglomeration of the fractured particles that impedes further fragmentation and, hence, size reduction; further, formation of surface cracks between the small aggregates or at the surface of individual particles could also have occurred [24].

As indicated previously, the relevance of adjusting the particle size lies on its effect on the electrical and mechanical properties of the nanocomposites. According to the literature, the nanoparticles agglomeration could adversely affect the electrical and mechanical properties of the nanocomposites [21, 22]. As the particle size decreases, the dispersion of the nanoparticles increases in the polymeric matrix and, therefore, improves the electrical and mechanical properties.

Scanning electron microscopy (SEM) images in **Figure 4** allow observing the dispersion of the nanoparticles in the polymer matrix. At low magnification, the presence of STO aggregates

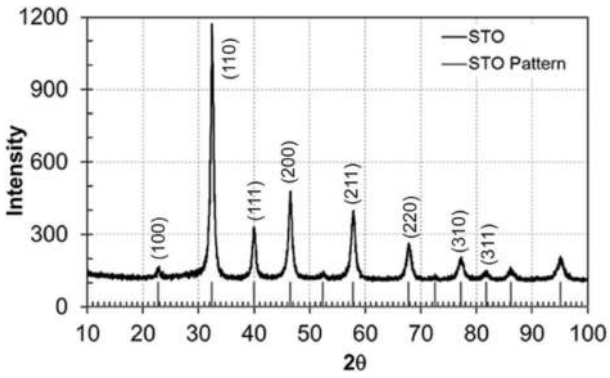

Figure 2. X-ray diffraction pattern of STO after 10 h of milling and powder diffraction line pattern.

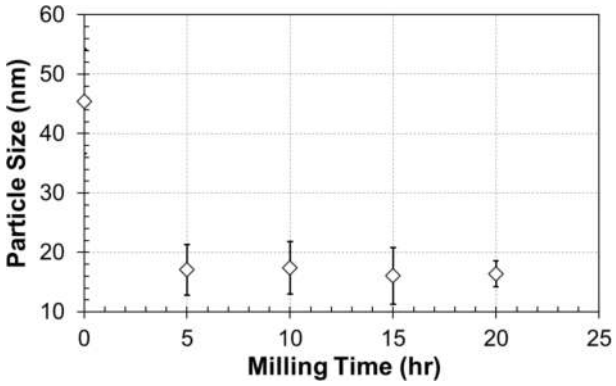

Figure 3. Particle size of STO nanoparticles at different milling times.

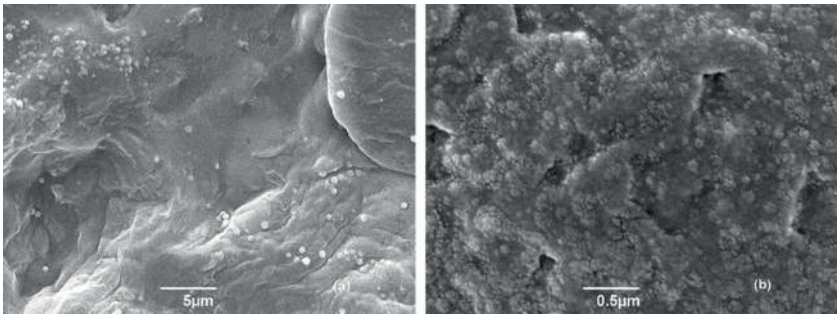

Figure 4. Secondary electron images obtained from the biocomposite with 20 wt% STO particles: (a) low magnification; (b) high magnification.

is apparent on the polymer surface. However, a significant dispersion of STO aggregates becomes visible on the polymer surface at high magnification.

3.2. Electrical properties

The dielectric constant was computed from the experimental results by using the capacitance equation for a parallel plate capacitor (Eq. (1)) at different frequencies. In a previous study, the addition of cellulose was detrimental to the capacitance of the nanocomposites while larger amounts of STO nanoparticles raised it [11]. Since the capacitance and the dielectric constant are directly proportional, higher amount of cellulose decreased the dielectric constant while the addition of the STO nanoparticles raised the dielectric constant of the nanocomposites (**Figure 5**). In addition, the dielectric constant of the nanocomposites diminished at high frequencies [25]. We expect that this finding will not only increase the capacity of energy storage devices but also control their capacitance values at different frequencies.

http://dx.doi.org/10.5772/intechopen.76858

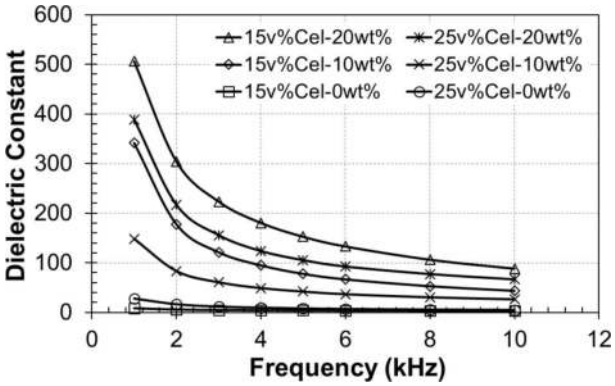

Figure 5. Calculated dielectric constant of the nanocomposites as a function of frequency.

As aforementioned, chitosan was dissolved in a water/acetic acid solution, enhancing the interaction between cellulose and water molecules in the solution. Such molecular interactions can be: (a) water molecules linked to cellulose hydroxyl (–OH) groups, or (b) water molecules confined between the polymer chains due to intermolecular hydrogen bonds. These interactions heightened the water content in the nanocomposites and, hence, raised the current flow through the capacitor [11, 26].

Moreover, higher amounts of STO nanoparticles increased the dielectric constant of the material [11]. The main characteristic of these ferroelectric nanoparticles consists of their ability to raise the material's stored energy. However, these ferroelectric nanoparticles are difficult to disperse in a polymeric matrix due to their high internal energy. It has also been reported that particle size reduction, by expanding the polymer-particles interface, enhanced the electrical properties of nanocomposites [11, 14].

Furthermore, the literature demonstrates how frequency alters the dipoles orientation of the STO nanoparticles [4–7]. When those nanoparticles are aligned with the applied electrical field, the dielectric material becomes polarized. However, the dipoles cannot remain aligned to the electrical field at higher frequencies [11]. In as much as the dielectric constant dwindles at those high frequencies, the polarization mechanism cannot contribute effectively to the dielectric properties. This represents a limitation because for higher frequencies applications this will cause decrease in the dielectric properties.

After analyzing the dielectric constant of the composites, we gaged the current density, i.e., charge transported through the cross-sectional area (**Figure 6**). Thus, we discovered that the current density raised for higher amounts of cellulose in the composites, as well as for voltages from 5 to 60 V. As explained previously, the water content of in the nanocomposites swells with the addition of cellulose, resulting in higher current densities through the dielectric material. Moreover, the STO nanoparticles addition improves the capacitor's ability to store more energy by lowering the current flow through the dielectric material. As shown in **Figure 6**, the current density for the composites with STO nanoparticles increased

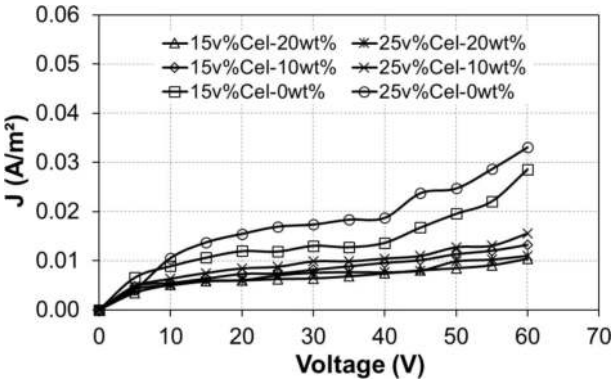

Figure 6. Effects of the applied electrical field, cellulose and STO nanoparticles content in the current density passing through the capacitors.

slightly [27]. Additionally, due to the fact that for safety reasons our instrumentation could only apply 60 V, we could not observe any breakdown in the composites up to that voltage. Not finding that breakdown voltage proves to be one limitation of the present research that could be overcome with a more energetic testing system. Yet, we strongly believe that the capacitors could withstand higher voltages with the addition of STO nanoparticles.

Furthermore, the electrical conductivity of the dielectric material was computed from the current density. For this calculation, a linear regression analysis was applied to the curves of current density as a function of voltage. The slope of the curve represented the conductivity divided by the thickness of the capacitor (σ_t). According to the results, higher content of cellulose heightened the conductivity of the dielectric material while the addition of STO nanoparticles lowered it (**Figure 7**). This is an important finding, since one can design capacitors by tuning the levels of cellulose and STO particles present in the biocomposite which are also in agreement with a recent study by Wang et al. [28].

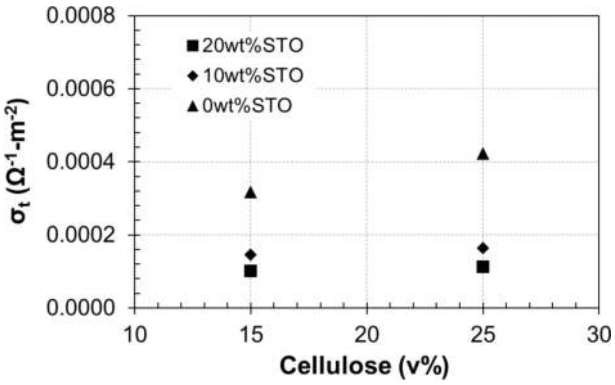

Figure 7. Effects of the cellulose and STO nanoparticles content in the electrical conductivity of the capacitors.

3.3. Thermal and tensile analysis

In this section, the thermal and mechanical properties of the composites were studied as a function of the cellulose percent, i.e., 15 and 25 v%, and the amount of strontium titanate nanoparticles, i.e., 0, 10 and 20 wt%.

As presented previously, the degradation temperature of the nanocomposites was analyzed via thermogravimetric analysis. Our results suggest that higher degradation temperature resulted from increasing the amount of cellulose in the composites bearing STO nanoparticles, which is opposite to the observed behavior for the composites without STO nanoparticles (**Figure 8**). In other words, the higher stability of the STO phase prevents early degradation (low T_{deg}) of the biocomposites. This outcome suggests that higher levels of both cellulose and STO could render these composites suitable for high temperature applications as in instrumentation operating in tropical regions.

In terms of mechanical behavior, the ultimate tensile strength (UTS) was determined using a uniaxial testing machine, as mentioned before. **Figure 9** reveals that higher UTS values were obtained in composites bearing more cellulose: from 15 to 25 v% for the composites containing STO nanoparticles, which is contrary to the behavior observed in composites without nanoparticles. When the UTS values for the composites are compared, the UTS values increased as the percentages of STO nanoparticles decreased from 20 to 0 wt%. We deem this an important finding as it enables the design of devices that can withstand minor loads without being mechanically ruptured upon service.

The addition of cellulose lowered slightly the T_{deg} and UTS for the composites without STO nanoparticles, an outcome attributed to the pH value of the solution. As shown in **Table 1**, the pH value for the composites without STO nanoparticles increased from 4.78 to 5.08. At higher pH values, the amino groups are protonated causing electrostatic repulsion between the polymer's chains [27]. Therefore, the electrostatic repulsions better the swelling degree of the polymer, as the water content heightens in the polymer [29]. Because of this apparent

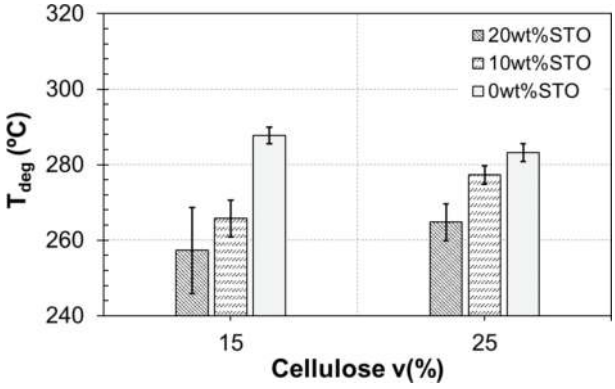

Figure 8. TGA analysis for composites made of 1.5v% chitosan/0.5v% cellulose considering 20, 10, and 0 wt% of strontium titanate nanoparticles.

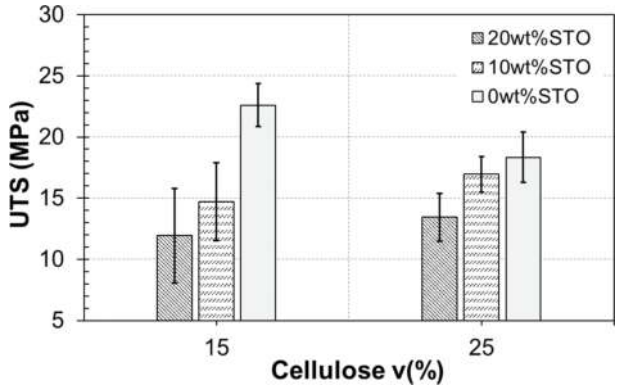

Figure 9. Tensile analysis for composites made of 1.5 v% chitosan/0.5 v% cellulose considering 20, 10 and 0 wt% of STO nanoparticles.

Percentage of cellulose (v%)	Percentage of STO nanoparticles (wt%)	pH value
15	0	4.78
15	10	4.78
15	20	5.00
25	0	5.08
25	10	5.08
25	20	5.20

Table 1. Measurements of pH value for the solutions containing different percentages of cellulose and STO nanoparticles.

shortcoming, when designing a device with these composites, one must consider this finding. Further testing of these composites under high humidity environment could shed light on the potential water absorption leading to swelling.

A different behavior was observed in the composites with STO nanoparticles where the T_{deg} and UTS increased. The polymer-polymer interaction and the polymer-particle interaction can be responsible of these results. The addition of STO nanoparticles could have furthered the entanglement of the polymer's chains and, consequently, the free volume. However, the water present in these free spaces can be removed during the drying process because the molecules of water are not confined between the polymer's chains.

In addition, the presence of more nanoparticles heightens the polymer-nanoparticles interfacial energy, which could cause cracks through the nanoparticles in the polymeric matrix. Besides, any agglomeration of nanoparticles can be detrimental for the polymer-nanoparticle interfacial bonding. Such agglomerates can favor the presence of pores and nucleate microspaces through the nanoparticles, raising the brittleness of the composites. All these are factors that require further experimentation, which falls beyond the scope of the present research.

All in all, we were able to establish a characterization baseline that can serve as design platform for capacitors intended to sustain high load at relatively elevated temperatures by adjusting the cellulose level and nanoparticles content. In closing, we are confident that this research would lead to the creation of organic and inexpensive tunable capacitors for RF applications like antennas or MEMS-based tunable filters.

4. Conclusions

The present work aimed at studying the electrical, thermal, and mechanical properties of composites made of chitosan, cellulose and strontium titanate nanoparticles. The compositional variables considered encompassed: cellulose content (15 and 25 v%) and amount of strontium titanate nanoparticles (10 and 20 wt%).

The chitosan-cellulose and polymer-nanoparticles composites were successfully fabricated via sol gel casting method. Strontium titanate nanoparticles were dispersed in the polymeric matrix using a double-layered technique. To achieve a better dispersion of the nanoparticles, the particles size was reduced from 43 to 18 nm using the high ball mill technique. As a result, a high dispersion of the nanoparticles in the polymeric matrix was achieved.

With respect to the measured electrical properties, the addition of the strontium titanate nanoparticles raised the dielectric constant, capacitance, and electrical resistivity of the composites, as expected from a dispersed dielectric material. Similarly, the addition of the nanoparticles decreased the current density passing through the biocomposite. In addition, the dielectric rupture of the composites was not observed up to a maximum applied voltage of 60 V.

Furthermore, mechanical and thermal analysis tests of the composites revealed that the addition of cellulose adversely affected the ultimate tensile strength and the degradation temperature of the composites without strontium titanate due to the high content of water. However, an opposing behavior was observed on the composites with strontium titanate nanoparticles, in which higher content of cellulose raised both the ultimate tensile strength and the degradation temperature while the addition of titanate nanoparticles lowered it.

Acknowledgements

Preliminary work on strontium titanate-containing biocomposites was published in an international journal [11]. This work is supported by the National Science Foundation under research Grant Nos. 0833112 and 1345156 (CREST program) and under instrumentation Grant Nos. 0619349 and 0922994. The authors would like to thank the invaluable assistance of the undergraduate student Javier Martínez and the technical personnel of the Materials Laboratories and Power Electronics Laboratories of the University of Puerto Rico-Mayagüez.: Dr. Eduardo I. Ortiz Rivera, and the students Daniel A. Merced Cirino and Alexander Collazo Irizarry.

Conflict of interest

The authors declare that there is no conflict of interest regarding the publication of this manuscript.

Author details

Amarilis Declet-Vega, Nelson Sepúlveda-Ramos and Oscar Marcelo Suárez*

*Address all correspondence to: oscarmarcelo.suarez@upr.edu

Nanotechnology Center for Biomedical, Environmental and Sustainability Applications, College of Engineering, University of Puerto Rico-Mayagüez, USA

References

[1] Dujardin BE, Mann S. Bio-inspired materials chemistry. Advanced Materials. 2002; **14**:775-788

[2] Shukla SK, Mishra AK, Arotiba OA, et al. Chitosan-based nanomaterials: A state-of-the-art review. International Journal of Biological Macromolecules. 2013;**59**:46-58

[3] Rinaudo M. Chitin and chitosan: Properties and applications. Progress in Polymer Science. 2006;**31**:603-632

[4] Kingery WD. Introduction to ceramics. Journal of the Electrochemical Society. 1977;**124**: 152C

[5] Carter CB, Norton MG. Ceramic Materials. 2nd ed. New York, USA: Springer-Verlag; 2013. Epub ahead of print 2013. DOI: 10.1016/S0026-0657(01)80220-4

[6] Neagu AM, Petronela L, Cazacu A, et al. Impedance analysis and tunability of $BaTiO_3$–chitosan composites: Towards active dielectrics for flexible electronics. Composites: Part B. 2014;**66**:109-116

[7] Elimat Z. AC-impedance and dielectric properties of hybrid polymer composites. Journal of Composite Materials. 2013;**49**:3-15

[8] Petrov I, Kalinkevich O, Pogorielov M, et al. Dielectric and electric properties of new chitosan-hydroxyapatite materials for biomedical application: Dielectric spectroscopy and corona treatment. Carbohydrate Polymers. 2016;**151**:770-778

[9] Hosokawa J, Nishiyama M, Yoshihara K, et al. Biodegradable film derived from chitosan and homogenized cellulose. Industrial and Engineering Chemistry Research. 1990;**29**:800-805

[10] Ibrahim MS, Sapuan SM, Faieza AA. Mechanical and thermal properties of composites from unsaturated polyester filled with oil palm ash. Journal of Mechanical Engineering Science. 2012;**2**:2231-8380

[11] Declet-Vega A, Sepúlveda-Ramos N, Martínez-Santos J, et al. Study of electrical properties of biocomposites containing ferroelectric nanoparticles. Journal of Composite Materials. 2017;**51**:1979-1985

[12] Holzwarth U, Gibson N. The Scherrer equation versus the 'Debye-Scherrer equation'. Nature Nanotechnology. 2011;**6**:534

[13] Alexander L, Klug HP. Determination of crystallite size with the X-ray spectrometer. Journal of Applied Physics. 1950;**21**:137-142

[14] Suárez OM, Vazquez J, Reyes-Russi L. Synthesis and characterization of mechanically alloyed Al/$Al_xMg_{1-x}B_2$ composites. Science and Engineering of Composite Materials. 2009;**16**:267-276

[15] Florián-Algarín D, Padilla A, Suárez OM, et al. Strengthening of Al and Al-Mg alloy wires by melt inoculation with Al/MgB_2 nanocomposite. Journal of the Mechanical Behavior of Materials. 2015;**24**:207-212

[16] Minteer TM. The many capacitance terms of two parallel discs in free space. European Journal of Physics. 2014;**35**:15

[17] ASTM-D-149. Standard test method for dielectric breakdown voltage and dielectric strength of solid electrical insulating materials at commercial power. ASTM International - Standards. 2013;**9**:1-13

[18] ASTM D150-11, Standard Test Methods for AC Loss Characteristics and Permittivity (Dielectric Constant) of Solid Electrical Insulation, ASTM International, West Conshohocken, PA, 2011. DOI: 10.1520/D0150-11

[19] Yang K, Huang X, Xie L, et al. Core-shell structured polystyrene/$BaTiO_3$ hybrid nanodielectrics prepared by in situ RAFT polymerization: A route to high dielectric constant and low loss materials with weak frequency dependence. Macromolecular Rapid Communications. 2012;**33**:1921-1926

[20] Barber P, Balasubramanian S, Anguchamy Y, et al. Polymer Composite and Nanocomposite Dielectric Materials for Pulse Power Energy Storage. 2009;**2**:1697-1733

[21] Burton AW, Ong K, Rea T, et al. On the estimation of average crystallite size of Zeolites from the Scherrer equation: A critical evaluation of its application to Zeolites with one-dimensional pore systems. Microporous and Mesoporous Materials. 2009;**117**:75-90

[22] Uvarov V, Popov I. Metrological characterization of X-ray diffraction methods for determination of crystallite size in nano-scale materials. Materials Characterization. 2007;**58**:883-891

[23] Trepakov VA, Potůček Z, Makarova MV, et al. $SrTiO_3$:Cr nanocrystalline powders: Size effects and optical properties. Journal of Physics. Condensed Matter. 2009;**21**:1-5

[24] Kelleher MC, Hashmi MSJ. The effect of vibratory milling on the powder properties of zinc oxide Varistors. Journal of Materials Processing Technology. 2008;**201**:645-650

[25] Wu Y, Guan K, Wang Z, et al. Isolation, Identification and Characterization of an Electrogenic Microalgae Strain. PLoS One. 2013;**8**:1-7

[26] Mazeau K. The hygroscopic power of amorphous cellulose: A modeling study. Carbohydrate Polymers. 2015;**117**:585-591

[27] Karthika R, Gopinath LR, Archaya S, et al. Isolation of diesel degrading bacteria, identification of catechol gene and its biogas production. IOSR Journal of Environmental Science, Toxicology and Food Technology. 2014;**8**:76-82

[28] Wang H, Fu Q, Luo J, et al. Three-phase Fe_3O_4 /MWNT/PVDF nanocomposites with high dielectric constant for embedded capacitor. Applied Physics Letters. 2017;**110**:242902

[29] Szymańska E, Winnicka K. Stability of chitosan—A challenge for pharmaceutical and biomedical applications. Marine Drugs. 2015;**13**:1819-1846